Transient exposure of carcinoma cells to RAS/MEK inhibitors and UCN-01 causes cell death *in vitro* and *in vivo*

Hossein Hamed,[1] William Hawkins,[1,4] Clint Mitchell,[1] Donna Gilfor,[1] Guo Zhang,[1] Xin-Yan Pei,[2] Yun Dai,[2] Michael P. Hagan,[3] John D. Roberts,[2] Adly Yacoub,[1,3] Steven Grant,[1,2] and Paul Dent[1,3]

Departments of [1]Biochemistry, [2]Medicine, [3]Radiation Oncology, and [4]Anatomy and Neurobiology, Virginia Commonwealth University, Richmond, Virginia

Abstract

The present studies were initiated to determine in greater molecular detail how MEK1/2 inhibitors [PD184352 and AZD6244 (ARRY-142886)] interact with UCN-01 (7-hydroxystaurosporine) to kill mammary carcinoma cells *in vitro* and radiosensitize mammary tumors *in vitro* and *in vivo* and whether farnesyl transferase inhibitors interact with UCN-01 to kill mammary carcinoma cells *in vitro* and *in vivo*. Expression of constitutively activated MEK1 EE or molecular suppression of JNK and p38 pathway signaling blocked MEK1/2 inhibitor and UCN-01 lethality, effects dependent on the expression of BAX, BAK, and, to a lesser extent, BIM and BID. *In vitro* colony formation studies showed that UCN-01 interacted synergistically with the MEK1/2 inhibitors PD184352 or AZD6244 and the farnesyl transferase inhibitors FTI277 and R115,777 to kill human mammary carcinoma cells. Athymic mice carrying ~100 mm^3 MDA-MB-231 cell tumors were subjected to a 2-day exposure of either vehicle, R115,777 (100 mg/kg), the MEK1/2 inhibitor PD184352 (25 mg/kg), UCN-01 (0.2 mg/kg), or either of the drugs in combination with UCN-01. Transient exposure of tumors to R115,777, PD184352, or UCN-01 did not significantly alter tumor growth rate or the mean tumor volume *in vivo* ~15 to 30 days after drug administration. In contrast, combined treatment with R115,777 and UCN-01 or with PD184352 and UCN-01 significantly reduced tumor growth. Tumor cells isolated after combined drug exposure exhibited a significantly greater reduction in plating efficiency using *ex vivo* colony formation assays than tumor cells that were exposed to either drug individually. Irradiation of mammary tumors after drug treatment, but not before or during treatment, significantly enhanced the lethal effects of UCN-01 and MEK1/2 inhibitor treatment. These findings argue that UCN-01 and multiple inhibitors of the RAS-MEK pathway have the potential to suppress mammary tumor growth, and to interact with radiation, *in vitro* and *in vivo*. [Mol Cancer Ther 2008;7(3):616–29]

Introduction

UCN-01 (7-hydroxystaurosporine) is currently being evaluated as an antineoplastic agent in clinical trials both alone and in combination with chemotherapeutic agents and ionizing radiation (1). UCN-01 exerts antiproliferative activity both *in vitro* and *in vivo*, an action that may be related to inhibition of protein kinase C isoforms (2). UCN-01 also enhances the cytotoxicity of chemotherapeutic agents by several postulated mechanisms, including inhibition of Chk1 (3). Inhibition of Chk1 may directly promote activation of the protein phosphatase Cdc25C and can also interfere with Cdc25C elimination by blocking its binding to 14-3-3 proteins and subsequent degradation (3). Down-regulation of Cdc25C results in enhanced phosphorylation and inactivation of cyclin-dependent kinases such as $p34^{cdc2}$, which are critically involved in G_2-M cell cycle arrest following DNA damage (4). More recently, UCN-01 has also been shown to inhibit the downstream effector of phosphatidylinositol 3-kinase, phosphoinositide-dependent protein kinase-1, in the same concentration range as protein kinase C isoforms (5). Thus, UCN-01 can func \tion as a checkpoint abrogator capable of enhancing the lethal actions of DNA-damaging agents, including ionizing radiation (6), cisplatin (7), ara-C (8), and camptothecins (9). It has generally been thought that UCN-01, administered at pharmacologically achievable concentrations, promotes cell death via cyclin-dependent kinase dephosphorylation rather than by inhibition of protein kinase C enzymes and phosphoinositide-dependent protein kinase-1 (10).

In the last 5 to 10 years, multiple growth factor receptors and downstream signal transduction pathways have been linked to the advantage tumor cells have over non-transformed cells in terms of increased rates of proliferation

Received 12/6/07; revised 1/12/08; accepted 1/18/08.

Grant support: USPHS grants R01-DK52825 and Department of Defense Award DAMD17-03-1-0262 (P. Dent); USPHS grants R01-CA100866, CA63753-06, and CA93738 (S. Grant); and The Jim Valvano ''Jimmy V'' Foundation. P. Dent is the holder of the Universal Inc. Professorship in Signal Transduction Research and S. Grant is the holder of the Olsen Distinguished Professorship.

The costs of publication of this article were defrayed in part by the payment of page charges. This article must therefore be hereby marked *advertisement* in accordance with 18 U.S.C. Section 1734 solely to indicate this fact.

Note: H. Hamed, W. Hawkins, and C. Mitchell contributed equally to this work.

Requests for reprints: Paul Dent, Department of Biochemistry, Virginia Commonwealth University, Box 980035, Richmond VA 23298-0035. Phone: 804-628-0861; Fax: 804-828-6042. E-mail: pdent@hsc.vcu.edu

Copyright © 2008 American Association for Cancer Research.

doi:10.1158/1535-7163.MCT-07-2376

Downloaded from http://aacrjournals.org/mct/article-pdf/7/3/616/1879092/616.pdf by guest on 07 October 2024

and cell survival following exposure to toxic stresses. Signaling by ErbB family and insulin-like growth factor-I receptors downstream into the ERK1/2, nuclear factor-κB, and, in particular, the phosphatidylinositol 3-kinase/phosphoinositide-dependent protein kinase-1/AKT pathways have been linked to the promotion of genomic instability, tumorigenesis, proliferation, and tumor cell resistance to cytotoxic therapeutic interventions. The ability of the ERK1/2 pathway to regulate proliferation versus differentiation and survival appears to depend on the amplitude and duration of ERK1/2 activation. A short activation of the ERK1/2 cascade has been correlated with enhanced progression through the G_1-S transition (11). In contrast, prolonged elevation of ERK1/2 activity has been shown to inhibit DNA synthesis through superinduction of the cyclin-dependent kinase inhibitor protein $p21^{CIP1}$, which may in turn lead to differentiation or to cell death (12). In addition to a role for ERK1/2 signaling in the G_1-S-phase transition, it has also been argued that ERK1/2 signaling may be involved in the ability of cells to progress through G_2-M, particularly following DNA damage–induced growth arrest (13, 14).

Multiple intracellular signal transduction pathways (e.g., ERK1/2 and phosphatidylinositol 3-kinase/AKT) are often highly activated in tumor cells and have been proposed as therapeutic targets in preventing cancer cell growth in many malignancies (e.g., refs. 15–17). Furthermore, inhibition of chemotherapeutic drug and radiation-induced growth factor receptor or signaling pathway activation by novel inhibitors of kinase domains has been shown by many groups to enhance the toxicity of established chemotherapy/radiation modalities (18–21). An alternative approach to killing tumor cells without the use of conventional cytotoxic agents is to exploit their reliance (that is, addiction) to high levels of signaling pathway activity to maintain growth and viability. Previous studies by this group have shown that UCN-01, at clinically relevant concentrations *in vitro*, causes activation of the ERK1/2 pathway in transformed cell types. Prevention of ERK1/2 pathway activation, by inhibition of either MEK1/2 or RAS function, rapidly promoted UCN-01-induced tumor cell death in a synergistic fashion (22–26). Nontransformed cells from multiple tissues were noted in several studies to be insensitive to apoptosis induction by this strategy. The concept that blocking compensatory survival pathway activation responses leads to tumor cell killing has been extended by our group and others using a variety of small-molecule inhibitors of kinases and other enzymes, including, for example, flavopiridol and phosphatidylinositol 3-kinase inhibitors; flavopiridol and histone deacetylase inhibitors; histone deacetylase inhibitors and perifosine; and MEK1/2 inhibitors and imatinib mesylate (27–30). The present studies determined whether farnesyl transferase inhibitors that inhibit RAS/RHO family function and downstream of RAS proteins, MEK1/2 inhibitors, interacted with UCN-01 in a synergistic fashion to suppress mammary tumor cell growth *in vivo*.

Materials and Methods

Materials

Phosphorylated/total ERK1/2 and anti-BAX antibodies were purchased from Cell Signaling Technologies. The anti-BAX monoclonal antibody 6A7 for immunoprecipitation of conformationally changed BAX was from Sigma-Aldrich. The anti-Ki67 antibody was purchased from Oncogene Research Products, anti-CD31/PECAM antibody was purchased from (Santa Cruz Biotechnology), and the cleaved caspase-3 antibody was purchased from Cell Signaling Technologies. All the secondary antibodies (anti-rabbit, anti-mouse, and anti-goat horseradish peroxidase) were purchased from Santa Cruz Biotechnology. Enhanced chemiluminescence and terminal deoxynucleotidyl transferase–mediated dUTP nick end labeling kits were purchased from NEN Life Science Products and Boehringer Mannheim, respectively. Trypsin-EDTA, RPMI, and penicillin-streptomycin were purchased from Life Technologies. MDA-MB-231, MCF7, HCT116, DLD1, HEPG2, HEP3B, MiaPaca2, and PANC1 cells were purchased from the American Type Culture Collection. SV40 large T mouse embryonic fibroblasts lacking expression of various proapoptotic BH3 domain proteins were kindly provided by Dr. S. Korsmeyer (Harvard University). Transformed PKR-like endoplasmic reticulum kinase (-/-) cells were kind gifts from the Ron Laboratory, Skirball Institute, New York University School of Medicine. FTI277, PD98059, and U0126 were purchased from Calbiochem/EMD Sciences. UCN-01 was generously provided by Keryx Biopharmaceuticals and the National Cancer Institute, NIH. AZD6244 (ARRY-142886) was generously provided by AstraZeneca Pharmaceuticals and the National Cancer Institute, NIH. R115,777 was generously provided by Johnson & Johnson Pharmaceutical Research and Development and the National Cancer Institute, NIH. Other reagents were as described in refs. 22–26.

Methods

Culture and *In vitro* Exposure of Cells to Drugs. Tumor cells for the studies in this article were cultured at 37°C [5% (v/v) CO_2] *in vitro* using RPMI supplemented with 10% (v/v) FCS. *In vitro* UCN-01/PD184352/AZD6244/U0126/PD98059/FTI277/R115,777 treatment was from a 100 mmol/L stock solution of each drug and the maximal concentration of vehicle (DMSO) in medium was 0.02% (v/v).

***In vitro* and *Ex vivo* Cell Treatments, SDS-PAGE, and Western Blot Analysis.** For *in vitro* analyses of short-term apoptosis effects, cells were treated with vehicle, UCN-01, PD184352/U0126/PD98059, or their combination for the indicated times. Cells for *in vitro* or *ex vivo* colony formation assays were plated at 250 to 4,000 per well in sextuplicate and for *in vitro* assays 14 h after plating were treated with either vehicle (DMSO), UCN-01 (10-150 nmol/L), PD184352 (0.1-2.0 μmol/L), AZD6244 (0.2-0.6 μmol/L), FTI277 (0.5-1.5 μmol/L), R115,777 (0.15-0.3 μmol/L), or the drug combination(s) for 48 h followed by drug removal. As indicated, in some assays, cells and tumors were irradiated after drug removal. Ten to 14 days after exposure or tumor

Downloaded from http://aacrjournals.org/mct/article-pdf/7/3/616/1879092/616.pdf by guest on 07 October 2024

isolation, plates were washed in PBS, fixed with methanol, and stained with a filtered solution of crystal violet (5%, w/v). After washing with tap water, the colonies were counted both manually (by eye) and digitally using a ColCount plate reader (Oxford Optronics). Data presented are the arithmetic mean ± SE from both counting methods from multiple studies. Colony formation was defined as a colony of ≥50 cells.

For SDS-PAGE and immunoblotting, cells were plated at $5 \times 10^5/cm^2$ and treated with PD184352/PD98059 and UCN-01 at the indicated concentrations and after the indicated time of treatment lysed for immunoprecipitations of BAX (23, 24) or with whole-cell lysis buffer [0.5 mol/L Tris-HCl (pH 6.8), 2% SDS, 10% glycerol, 1% β-mercaptoethanol, 0.02% bromophenol blue], and the samples were boiled for 30 min. The boiled samples were loaded onto 10% to 14% SDS-PAGE and electrophoresis was run overnight. Proteins were electrophoretically transferred onto 0.22 μm nitrocellulose and immunoblotted with various primary antibodies against different proteins. All immunoblots were visualized by enhanced chemiluminescence.

***In vivo* Exposure of Mammary Carcinoma Tumors to Drugs.** Athymic female NCr-*nu/nu* mice were obtained from The Jackson Laboratory. Mice were maintained under pathogen-free conditions in facilities approved by the American Association for Accreditation of Laboratory Animal Care. MDA-MB-231 cells were cultured and isolated by trypsinization followed by cell number determination using a hemacytometer. Cells were resuspended in PBS and 5 million tumor cells/100 μL PBS were injected into the right rear flank of each mouse, and tumors were permitted to form to a volume of ~100 mm^3 over the following 3 to 4 weeks. PD184352 was aliquoted into ~50 mg/vial and stored in a -20°C cold room under vacuum and protected from light. For animal administration, PD184352 was first dissolved in DMSO; the amount of microliter of DMSO used was four times the number of milligram of PD184352 to be dissolved (that is, 50 mg in 200 μL DMSO). Next, an equal volume of Cremophor (Sigma) was added. After mixing, a 1:10 dilution was made with 0.9% sterile saline. Animals were i.p. injected with PD184352 to a final concentration of 25 mg/kg body mass. Animals received two more injections of PD184352, 8 h apart for 2 days. R115777 was freshly prepared in 2% (w/v) β-cyclodextrin in 0.1 N HCl followed by dilution into an equal volume of Cremophor (Sigma) and a 1:10 dilution was made with 0.9% sterile saline for a final dose of 100 mg/kg body mass, once daily for 2 days. UCN-01 was administered 45 min after the first PD184352 injection each day for 2 days. UCN-01 was diluted in a solution of 2% (w/v) sodium citrate (pH 3.5). An aliquot of diluent was filter sterilized using a 10 mL syringe and 0.2 μm filter. The UCN-01 was further diluted 1:20 with sodium citrate, and animals were injected i.p. for a final concentration of 0.2 mg/kg. Each animal not receiving a dose of PD184352 or UCN-01 at the time of drug treatment was given an i.p. injection of diluent alone in a volume equal to the amount given with the drug. Tumor volumes were calculated from the formula: $(l \times w^2) / 2$, where l and w are longest and shortest lengths, respectively, of the tumor. Tumor growth was expressed as relative fold change in tumor volume, (T_x / T_0), where T is the mean tumor volume of all tumors at a particular time in days x and T_0 was the mean tumor volume at day 0.

***Ex vivo* Manipulation of Mammary Carcinoma Tumors**

Animals were euthanized by CO_2 and placed in a BL2 cell culture hood on a sterile barrier mat. The bodies of the mice were soaked with 70% (v/v) ethanol and the skin around the tumor was removed using small scissors, forceps, and a disposable scalpel. These implements were flame sterilized between removal of the outer and inner layers of skin. A piece of the tumor (~50% by volume) was removed and placed in a 10-cm dish containing 5 mL RPMI on ice. In parallel, the remainder of the tumor was placed in 5 mL Streck Tissue Fixative (Fisher Scientific) in a 50 mL conical tube for fixation; H&E staining of fixed tumor sections was done as described (31). The tumor sample that had been placed in RPMI was minced with a sterile disposable scalpel into the smallest possible pieces and then placed in a sterile disposable flask. The dish was rinsed with 6.5 mL RPMI, which was then added to the flask. A 10× solution of collagenase (Sigma; 2.5 mL, 28 units/mL final concentration) and 10× enzyme mixture containing DNase (Sigma; 308 units/mL final concentration) and Pronase (EMD Sciences; 22,500 units/mL final concentration) in a volume of 1 mL was added to the flask. The flasks were placed into an orbital shaking incubator at 37°C for 1.5 h at 150 rpm. Following digestion, the solution was passed through a 0.4 μm filter into a 50 mL conical tube. After mixing, a sample was removed for viable and total cell counting using a hemacytometer. Cells were centrifuged at $500 \times g$ for 4 min, the supernatant was removed, and fresh RPMI containing 10% (v/v) FCS was added to give a final resuspended cell concentration of 1×10^6 cells/mL. Cells were diluted and plated in 10 cm dishes in triplicate at a concentration of 2×10^3 per dish for control and individual drug treatments and 4×10^3 per dish for combined drug exposures (22).

Immunohistochemistry and Staining of Fixed Tumor Sections. Fixed tumors were embedded in paraffin wax and 10 μm slices were obtained using a microtone. Tumor sections were deparafinized and rehydrated and antigen retrieval was done in a 10 mmol/L (w/v) sodium citrate/citric acid buffer (pH 6.7) heated to 90°C in a constant temperature microwave oven. Prepared sections were then blocked and subjected to immunohistochemistry as per the instructions of the manufacturer for each primary antibody (phosphorylated ERK1/2; Ki67; CD31; cleaved caspase-3). The tissue sections were dehydrated, cleared, and mounted with coverslips using Permount. The permanently mounted slides were allowed to dry overnight and photographed at the indicated magnification. The area selected for all photomicrographs was the proliferative zone, within 2 mm of or juxtaposed to leading edge of the tumor.

Short-term Cell Viability Assays after Drug Exposure. Cells were isolated at the indicated times by trypsinization

Downloaded from http://aacrjournals.org/mct/article-pdf/7/3/616/1879092/616.pdf by guest on 07 October 2024

Table 1. PD184352, AZD6244, and multiple farnesyl transferase inhibitors synergize with UCN-01 *in vitro* to kill MDA-MB-231 cells as measured in colony formation assays

UCN-01 (nmol/L)	PDI84352 (μmol/L)	Fraction affected	CI
22.5	0.3	0.35	0.34
30.0	0.4	0.38	0.61
37.5	0.5	0.46	0.63
UCN-01 (nmol/L)	AZDG244 (μmol/L)	Fraction affected	CI
25	0.2	0.25	0.51
50	0.4	0.32	0.61
75	0.6	0.39	0.69
UCN-01 (nmol/L)	R115,777 (μmol/L)	Fraction affected	CI
25	0.150	0.23	0.55
37.5	0.225	0.36	0.59
50	0.300	0.41	0.65
UCN-01 (nmol/L)	FTI277 (μmol/L)	Fraction affected	CI
37.5	0.5	0.38	0.26
75	1.0	0.42	0.47
112.5	1.5	0.46	0.57

NOTE: MDA-MB-231 cells were plated as single cells in sextuplicate for colony formation assays as described in Materials and Methods. Cells were permitted to attach at 12 h after plating and each well was treated for 48 h with the indicated concentrations of PD184352, AZD6244, R115,777, FTI277, and UCN-01. Following 48 h of drug treatment, the medium was carefully removed, the cells were washed with medium, and fresh medium lacking drugs was added to the cultures. Colonies of cells were permitted to form for the following 10 to 14 d. Cells were fixed, stained, and counted both manually by eye and using a ColCount machine (Oxford Optronics). A colony is defined as >50 cells. The mean ± SE colony numbers from both methods of counting were used to calculate plating efficiency for each condition. Median dose effect isobologram analyses with the drug treatments at a fixed ratio were done using CalcuSyn software (Biosoft). A CI of <1.00 indicates synergy, whereas a CI of >1.00 indicates antagonism. Data are a representative experiment (n = 3).

and either subjected to trypan blue cell viability assay by counting in a light microscope or fixed to slides and stained using a commercially available Diff Quick (Geimsa) assay kit (22–24). The Annexin V/propidium iodide assay was carried to determine cell viability out as per the manufacturer's instructions (BD PharMingen) using a Becton-Dickinson FACScan flow cytometer.

Data Analysis. Comparison of the effects of various *in vivo* treatments was done using a random-effects mixed model with an AR(1) error covariance structure. Tumor growth data shown in each figure are the mean ± SE of one representative experiment using six to nine animals per treatment condition from multiple (three to four) separate studies. Comparison of the effects between various *in vitro* drug treatments was done following ANOVA using the Student's t test. Differences with $P < 0.05$ were considered statistically significant. Experiments shown are the mean ± SE of multiple individual points from multiple studies. Median dose effect isobologram colony formation analyses to determine synergism of drug interaction were done according to the methods of Chou and Talalay using the CalcuSyn program for Windows (Biosoft). Cells were treated with agents at an escalating fixed concentration drug dose. A combination index (CI) of <1.00 indicates synergy of interaction between the two drugs; a CI of ~1.00 indicates an additive interaction; a CI of >1.00 indicates antagonism of action between the agents.

Results

Initial studies showed that the MEK1/2 inhibitor PD184352 and UCN-01 interacted in a synergistic manner to kill mammary tumor cells *in vitro* (22). A 48-h exposure of either MDA-MB-231 or MCF7 cells to PD184352 and UCN-01 resulted in a synergistic induction of cell killing as measured ~14 days after drug removal in colony formation assays (Tables 1 and 2). A CI of <1.00 indicates a toxic synergy of interaction between the drugs when survival data are calculated within this computational assay. Very similar CI data (that is, <1.00) were obtained when the

Table 2. PD184352, AZD6244, and multiple farnesyl transferase inhibitors synergize with UCN-01 to kill MCF7 cells as measured in colony formation assays

UCN-01 (nmol/L)	PD184352 (μmol/L)	Fraction affected	CI
22.5	0.30	0.09	0.60
30.0	0.40	0.13	0.66
37.5	0.50	0.22	0.61
UCN-01 (nmol/L)	AZD6244 (μmol/L)	Fraction affected	CI
20.0	0.20	0.08	0.71
25.0	0.25	0.15	0.73
30.0	0.30	0.18	0.70
UCN-01 (nmol/L)	R115,777 (μmol/L)	Fraction affected	CI
25	0.150	0.53	0.51
37.5	0.225	0.66	0.40
50	0.300	0.74	0.33
UCN-01 (nmol/L)	FTI277 (μmol/L)	Fraction affected	CI
37.5	0.5	0.29	0.46
75	1.0	0.33	0.76
112.5	1.5	0.42	0.77

NOTE: MCF7 cells were plated as single cells in sextuplicate for colony formation assays as described in Materials and Methods. Cells were permitted to attach at 12 h after plating and each well was treated for 48 h with the indicated concentrations of PD184352, AZD6244, R115,777, FTI277, and UCN-01. Following 48 h of drug treatment, the medium was carefully removed, the cells were washed with medium, and fresh medium lacking drugs was added to the cultures. Colonies of cells were permitted to form for the following 10 to 14 d. Cells were fixed, stained, and counted both manually by eye and using a ColCount machine (Oxford Optronics). A colony is defined as >50 cells. The mean ± SE colony numbers from both methods of counting were used to calculate plating efficiency for each condition. Median dose effect isobologram analyses with the drug treatments at a fixed ratio were done using CalcuSyn software (Biosoft). A CI of <1.00 indicates synergy, whereas a CI value of >1.00 indicates antagonism. Data are a representative experiment (n = 3).

Downloaded from http://aacrjournals.org/mct/article-pdf/7/3/616/1879092/616.pdf by guest on 07 October 2024

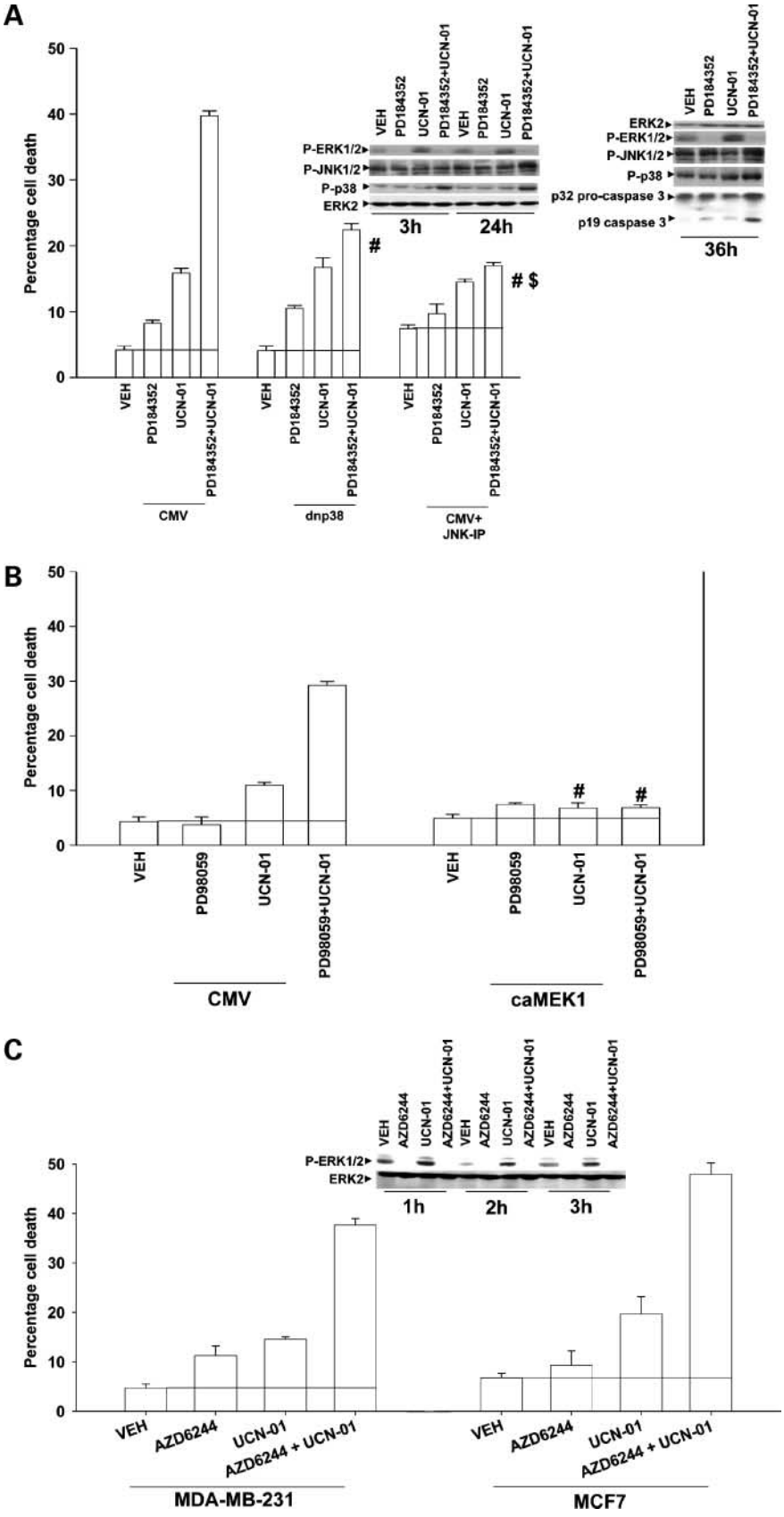

Figure 1. UCN-01 activates ERK1/2 that is blocked by the MEK1/2 inhibitor PD184352, which correlates with activation of JNK1/2 and p38 MAPK and the induction of tumor cell death. MDA-MB-231 cells were cultured as described in Materials and Methods (22). **A,** top, MDA-MB-231 cells were treated with vehicle control (DMSO) or with UCN-01 (150 nmol/L), PD184352 (1 μmol/L), or both drugs. Cells were isolated at the indicated times after treatment, lysed, and subjected to SDS-PAGE followed by immunoblotting to determine the phosphorylation of ERK1/2, JNK1/2, and p38 MAPK as well as total ERK2 and caspase-3 levels (n = 3). Bottom, MDA-MB-231 cells were cultured as described in Materials and Methods (22). Twelve hours after plating, cells were infected with either a control empty vector adenovirus (*CMV*) or an adenovirus to express dominant-negative p38α MAPK at a multiplicity of infection of 30. Twenty-four hours after infection, cells were pretreated with vehicle (DMSO) or JNK inhibitory peptide (*JNK-IP*; 10 μmol/L) as indicated and 30 min later treated with vehicle control (*VEH*; DMSO) or with UCN-01 (150 nmol/L), PD184352 (1 μmol/L), or both drugs. Cells were isolated 48 h after treatment and the percentage cell death was determined in triplicate from two separate experiments ± SE using trypan blue exclusion assays. **B,** MDA-MB-231 cells were cultured as described in Materials and Methods (22). Twelve hours after plating, cells were infected with either a control empty vector adenovirus or an adenovirus to express constitutively active MEK1 EE at a multiplicity of infection of 30. Twenty-four hours after infection, cells were treated with vehicle control (DMSO) or with UCN-01 (150 nmol/L), PD98059 (25 μmol/L), or both drugs. Cells were isolated 48 h after treatment and the percentage cell death was determined in triplicate from two separate experiments ± SE using trypan blue exclusion assays. **C,** MDA-MB-231 and MCF7 cells were cultured as described in Materials and Methods (22). Twenty-four hours after plating, cells were treated with vehicle control (DMSO) or with UCN-01 (150 nmol/L), AZD6244 (0.2 μmol/L), or both drugs. Cells were isolated 48 h after treatment and the percentage cell death was determined in triplicate from two separate experiments ± SE using trypan blue exclusion assays. Top, MCF7 cells were treated with vehicle control (DMSO) or with UCN-01 (150 nmol/L), AZD6244 (0.2 μmol/L), or both drugs simultaneously. Cells were isolated after treatment and subjected to SDS-PAGE and blotting to determine ERK1/2 phosphorylation and total ERK2 levels (n = 2).

Downloaded from http://aacrjournals.org/mct/article-pdf/7/3/616/1879092/616.pdf by guest on 07 October 2024

novel MEK1/2 inhibitor AZD6244 was substituted for PD184352 in the colony formation/isobologram assays (Tables 1 and 2).

As observed previously, treatment of MDA-MB-231 and MCF7 cells *in vitro* with UCN-01 caused ERK1/2 activation that was blocked by the MEK1/2 inhibitor PD184352 (Fig. 1A, *top*). Other findings revealed that treatment of cells with UCN-01 and PD184352 promoted activation of p38 MAPK and JNK1/2 that correlated with pro-caspase-3 cleavage (22, 23). Inhibition of JNK1/2 function and to a lesser extent p38 MAPK function suppressed the lethality of the UCN-01 and PD184352 drug combination treatment (Fig. 1A). To determine whether inhibition of MEK1/2 was truly involved in the interaction between UCN-01 and PD184352 in breast cancer cells, we made use of the MEK1/2 inhibitor PD98059, which weakly inhibits the function of constitutively activated MEK1 EE, in contrast to the MEK1/2 inhibitor PD184352. PD98059 enhanced the toxicity of

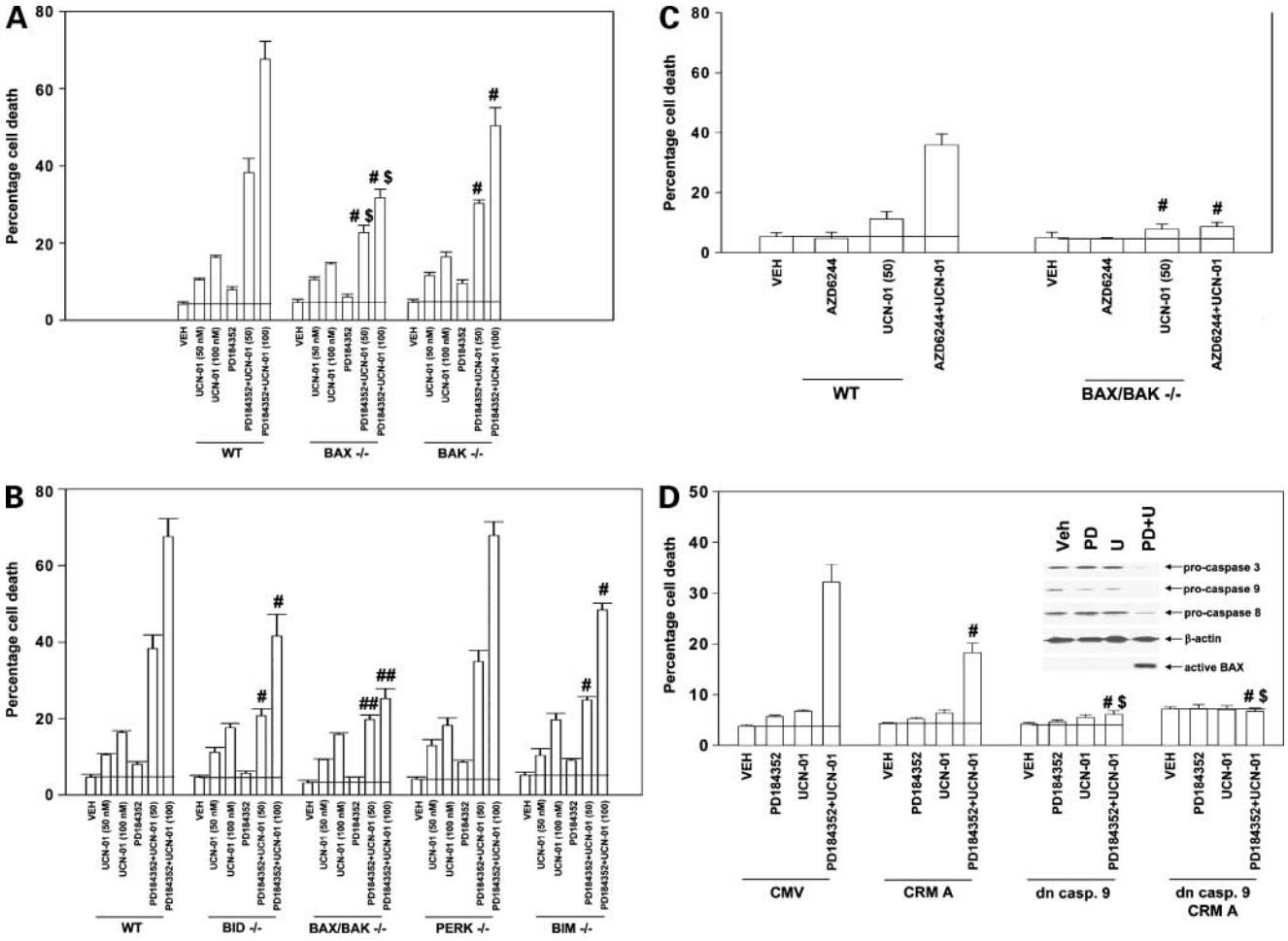

Figure 2. MEK1/2 inhibitors interact with UCN-01 to synergistically promote cell death in transformed cells that is blocked by loss of BAX and BAK function and by inhibition of caspase-9 and caspase-8 function. **A,** transformed mouse embryonic fibroblasts were treated with vehicle (DMSO), PD184352 (1 μmol/L), UCN-01 (50 nmol/L; 100 nmol/L), or the drug combination. Cells were isolated 48 h after treatment and the percentage cell death was determined in triplicate from two separate experiments ± SE using trypan blue exclusion assays. #, $P < 0.05$, less than corresponding value in wild-type cells; $, $P < 0.05$, less than corresponding value in BAK-/- cells. **B,** transformed mouse embryonic fibroblasts were treated with vehicle (DMSO), PD184352 (1 μmol/L), UCN-01 (50 nmol/L; 100 nmol/L), or both drugs. Cells were isolated 48 h after treatment and the percentage cell death was determined in triplicate from two separate experiments ± SE using trypan blue exclusion assays. #, $P < 0.05$, less than corresponding value in wild-type cells; ##, $P < 0.05$, less than corresponding value in BAX-/- cells. **C,** transformed mouse embryonic fibroblasts were treated with vehicle (DMSO), AZD6244 (0.2 μmol/L), UCN-01 (50 nmol/L), or both drugs. Cells were isolated 48 h after treatment and the percentage cell death was determined in triplicate from two separate experiments ± SE using trypan blue exclusion assays. #, $P < 0.05$, less than corresponding value in wild-type cells. **D,** MDA-MB-231 cells were cultured as described in Materials and Methods (22). Twelve hours after plating, cells were infected with either a control empty vector adenovirus, an adenovirus to express the caspase-8 inhibitor CRM A, or an adenovirus to express dominant-negative caspase-9. Twenty-four hours after infection, cells were treated with vehicle control (DMSO) or with UCN-01 (150 nmol/L), PD184352 (1 μmol/L), or both drugs. Cells were isolated 48 h after treatment and the percentage cell death was determined in triplicate from two separate experiments ± SE using trypan blue exclusion assays. Top inset, MDA-MB-231 cells were treated with vehicle control (DMSO), PD98059 (25 μmol/L), UCN-01 (150 nmol/L), or both drugs. Cells were isolated 24 h after drug exposure and immunoblotting was done to show the cleavage/integrity status of pro-caspase-3, pro-caspase-8, and pro-caspase-9 and the conformational activity change in BAX (after prior immunoprecipitation).

Downloaded from http://aacrjournals.org/mct/article-pdf/7/3/616/1879092/616.pdf by guest on 07 October 2024

UCN-01 in MDA-MB-231 cells, which was suppressed by expression of a constitutively active MEK1 EE protein (Fig. 1B). In general agreement with our colony formation assays, exposure of breast cancer cells to UCN-01 and AZD6244 enhanced cell killing in a greater than additive fashion in short-term viability assays (Fig. 1C). Exposure of a variety of cancer cell types to UCN-01 and AZD6244 also enhanced cell killing in a greater than additive fashion in short-term viability assays (Supplementary Figs. S1 and S2).[5] The only tumor cell type that appeared to be resistant to this drug regimen were melanoma cells that either lacked expression of or had reduced expression of Apaf-1 (data not shown).

Additional studies then attempted to define more precisely the molecular mechanisms by which cell killing occurred. Treatment of SV40 large T antigen transformed mouse embryonic fibroblasts with PD184352 and UCN-01 caused a dose-dependent increase in cell killing that was suppressed in BAK-/- cells and to a greater extent in BAX-/- cells (Fig. 2A). Loss of BAX and BAK expression nearly abolished the toxic interaction between PD184352 and UCN-01 and between AZD6244 and UCN-01 (Fig. 2B and C). The loss of both BID and BIM expression, but not that of PKR-like endoplasmic reticulum kinase, also suppressed the toxic interaction between PD184352 and UCN-01 (Fig. 2B). Treatment of MDA-MB-231 cells *in vitro* with MEK1/2 inhibitors and UCN-01 correlated with the cleavage of pro-caspase-9, pro-caspase-8, and pro-caspase-3 and altered BAX conformation (Fig. 2D, *top inset*). In general agreement with prior data using small-molecule caspase inhibitors, apoptosis was partially blocked by expression of either the caspase-8 inhibitor CRM A or expression of dominant-negative caspase-9 and abolished by expression of both caspase inhibitors (Fig. 2D). Overexpression of BCL-XL abolished enhanced cell killing by AZD6244 and UCN-01 that was reverted by incubation with a commercially available BCL-2/BCL-XL inhibitor HA14-1 (Supplementary Fig. S3).[5] Thus, mitochondrial dysfunction and activation of the intrinsic apoptosis pathway appear to represent primary events in the killing process induced by MEK1/2 inhibitors and UCN-01 exposure.

To reevaluate whether our *in vitro* observations could be translated into an animal model system, athymic mice were injected in the rear flank with MDA-MB-231 cells and tumors were permitted to form. Mice bearing ~100 to 150 mm^3 tumors were then injected i.p. with vehicle, PD184352, UCN-01, or the drug combination for 2 days, and tumor volume was then measured over the following ~30 days. In general agreement with *in vitro* data, PD184352 suppressed basal and UCN-01-stimulated ERK1/2 phosphorylation *in vivo* (Fig. 3A). Thirty days following drug exposure, no statistically significant change in tumor volume was noted comparing vehicle-treated, PD184352-treated, or UCN-01-treated tumors (Fig. 3B, *left*). In contrast to data using individual drug treatments, combined treatment of animals with PD184352 and UCN-01 significantly reduced tumor growth ($P < 0.05$). Similar data were also obtained in tumors generated from MCF7 cells (data not shown). Tumors exposed to the drugs individually compared with vehicle control exhibited a reduced number of cells per field under H&E staining and a modest reduction in the levels of Ki67 immunoreactivity (Fig. 3B, *top right*). In contrast to our findings with individual drugs, combined exposure to PD184352 and UCN-01 caused a profound reduction in tumor cellularity and almost abolished Ki-67 immunoreactivity, indicative that tumor re-growth had been suppressed. These findings were supported by reduced survival of tumor cells in *ex vivo* colony formation assays (Table 3). Tumors exposed to both PD184352 and UCN-01 also appeared to have less CD31 immunoreactivity, suggesting that combined drug treatment had inhibited angiogenesis and/or killed tumor endothelial cells. Also in contrast to our findings with individual drug exposure, combined exposure to PD184352 and UCN-01 caused a rapid increase in immunoreactivity for the cleaved form of caspase-3, indicative of apoptosis (Fig. 3B, *bottom right*). Thus, MEK1/2 inhibitors enhance UCN-01 toxicity *in vivo*.

Radiotherapy is a primary modality used in the treatment of mammary carcinoma both *in situ* and at distant metastatic sites. Based on our findings in Fig. 3, we did additional studies to examine the response of PD184352- and UCN-01-treated tumors to ionizing radiation exposure during and following cessation of drug treatment. *In vitro*, irradiation of PD184352- and UCN-01-treated tumors after drug exposure and removal of the drugs from the growth medium enhanced cell death (Fig. 4A). *In vivo*, irradiation of PD184352- and UCN-01-treated tumors during drug exposure did not further enhance the toxic effects of drug exposure (Fig. 4B, *top left*). In contrast, irradiation of drug-treated tumors 24 h after the cessation of drug administration, after drug clearance, significantly enhanced the toxicity of radiation exposure (Fig. 4B, *bottom left*). The tumoricidal effects observed in Fig. 4B (*bottom*) correlated with increased cleavage of pro-caspase-3, reduced Ki67 immunoreactivity, and lower tumor cellularity (Fig. 4C). The tumoricidal actions of drug treatment and radiation exposure were in general agreement with *in vitro* colony formation assays in which tumor cells were treated with drugs followed by radiation exposure (Supplementary Fig. S4).[5] Collectively, these findings show in a xenograft model that ionizing radiation can be rationally combined following PD184352 (a MEK1/2 inhibitor) and UCN-01 treatment.

The Raf-MEK-ERK pathway is generally believed to signal downstream of growth factor receptors and the RAS proto-oncogene. Prior studies in human leukemia cells have shown that inhibitors of RAS protein lipid modification, farnesyl transferase inhibitors, statins, can suppress lipid modification of RAS and RHO family proteins and promote UCN-01 toxicity (32, 33). In human

[5] Supplementary material for this article is available at Molecular Cancer Therapeutics Online (http://mct.aacrjournals.org/).

Downloaded from http://aacrjournals.org/mct/article-pdf/7/3/616/1879092/616.pdf by guest on 07 October 2024

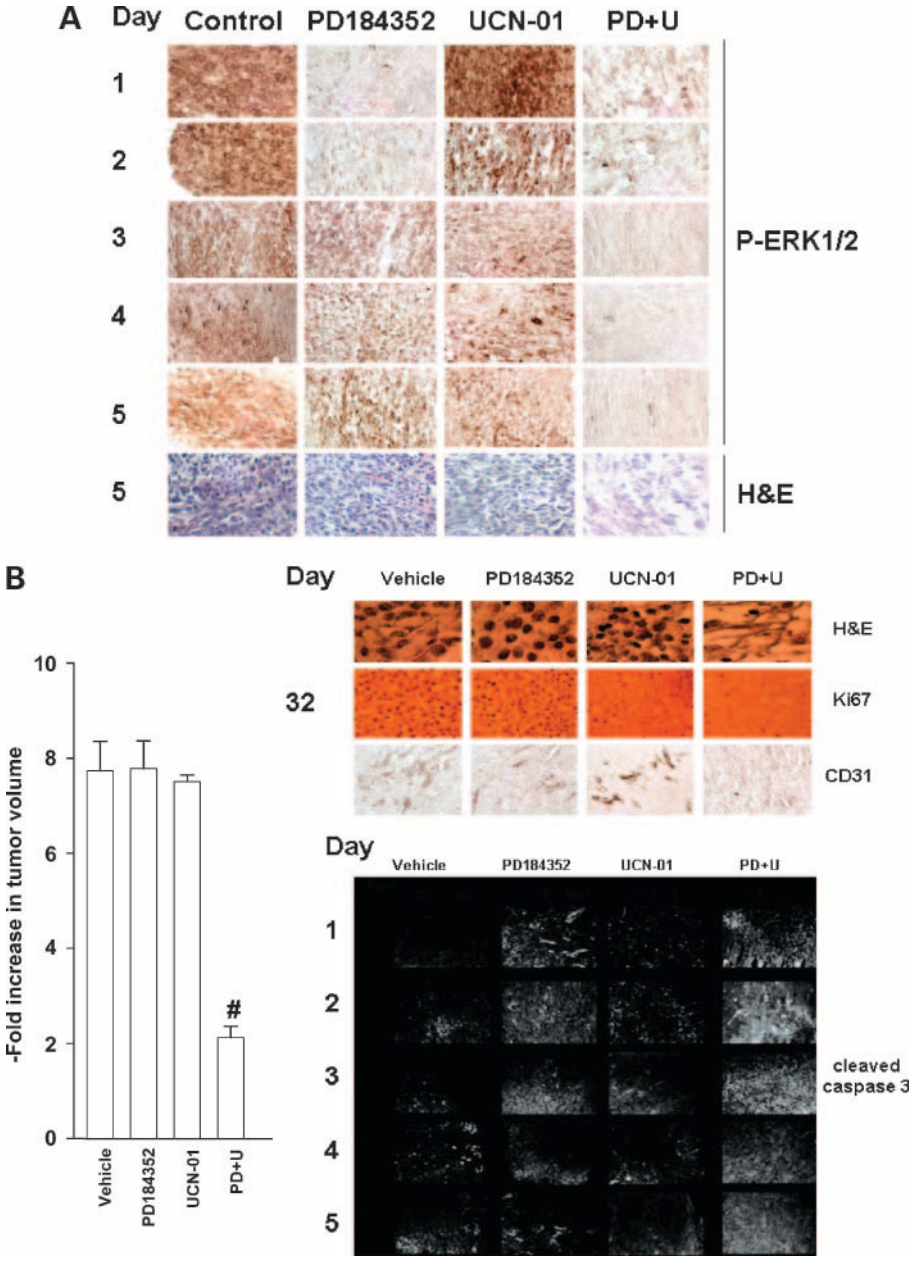

Figure 3. PD184352 and UCN-01 combine to suppress the growth of established estrogen-independent MDA-MB-231 mammary carcinoma tumors in a greater than additive fashion. **A,** animals were injected 5 million cells/100 μL PBS female athymic mice s.c. into the rear flank: tumor take rate was >90%. Tumors were permitted to form for the following 20 d. Animals with palpable tumors (~100 mm^3) were sorted with the intention of providing a normal distribution of tumor volume within each group, so that the mean tumor volume of all animals within a group was within 10%. Animals were injected with vehicle, PD184352, UCN-01, or the drug combination for 2 d as described in Materials and Methods. At the indicated d after the start of drug treatment, the tumors were isolated and fixed and 10 μm sections were taken for H&E and immunohistochemical staining to determine ERK1/2 phosphorylation/immunoreactivity. Images, except where indicated, were taken at ×60 magnification using a Olympus microscope. Representative of three independent tumors. **B,** animals were injected 5 million cells/100 μL PBS female athymic mice s.c. into the rear flank: tumor take rate was >90%. Tumors were permitted to form for the following 20 d. Animals with palpable tumors (~100 mm^3) were sorted with the intention of providing a normal distribution of tumor volume within each group, so that the mean tumor volume of all animals within a group was within 10%. Animals were injected with vehicle, PD184352, UCN-01, or the drug combination for 2 d as described in Materials and Methods. Tumors were calipered to determine their volume calculated as (width^2) × length / 2, where width is the smaller of the two measurements. Left, mean ± SE tumor volume for all animals in each treatment condition was plotted 30 d after cessation of drug exposure (n = 8). #, $P < 0.05$, less than vehicle control value. Representative of four independent studies. Right, as indicated, 32 d after treatment, portions of the tumors were fixed and 10 μm sections were taken for H&E and immunohistochemical staining to determine morphology, cellularity, and Ki67 and CD31 immunoreactivity. Images, except where indicated, were taken at ×60 magnification using a Olympus microscope. Representative of three tumors. At the indicated days after the start of drug treatment (days 1-5), the tumors were isolated and fixed and 10 μm were sections taken for immunohistochemical staining to determine reactivity for the cleaved form of caspase-3. Images, except where indicated, were taken at ×60 magnification using an Olympus microscope. Representative of three tumors.

Downloaded from http://aacrjournals.org/mct/article-pdf/7/3/616/1879092/616.pdf by guest on 07 October 2024

Table 3. ***Ex vivo*** **colony formation assays from MDA-MB-231 tumors treated with UCN-01 and other signaling modulatory agents**

Vehicle	PD184352	UCN-01	PD184352 + UCN-01
1.00	0.83 ± 0.12	0.81 ± 0.06 (1.00)	0.31 ± 0.06 (0.38*)
Vehicle	R115,777	UCN-01	R115,777 + UCN-01
1.00	0.79 ± 0.05	0.83 ± 0.07 (1.00)	0.40 ± 0.04 (0.48*)
Vehicle	PD184352 + UCN-01	Vehicle then 2 Gy	PD184352 + UCN-01 then 2 Gy
1.00	0.28 ± 0.06	0.26 ± 0.03 (1.00)	0.04 ± 0.01 (0.15*)

NOTE: Tumors were treated with the indicated agents as described in Materials and Methods, and 30 d after cessation of drug treatment, the animals were humanely sacrificed and the tumors were isolated. Individual MDA-MB-231 cells were isolated from the tumors and then plated in sextuplicate as single cells for colony formation assays as described in Materials and Methods. Colonies were permitted to form for the following 10 to 14 d. Cells were fixed, stained, and counted both manually and using a ColCount machine (Oxford Optronics). The mean ± SE colony numbers from both methods of counting were used to calculate plating efficiency for each treatment condition. Data shown in parentheses indicate cell survival for cells treated with UCN-01, with survival for UCN-01 normalized to 1.00. Data are from a representative experiment ($n = 3$).

*$P < 0.05$ less than single drug exposure.

mammary carcinoma cells, the farnesyl transferase inhibitors FTI277 and R115,777 interacted synergistically with UCN-01 to kill MDA-MB-231 and MCF7 cells *in vitro* (Tables 1 and 2). Treatment of MDA-MB-231 cells with R115,777 inhibited UCN-01-stimulated activation of ERK1/2 but did not suppress basal ERK1/2 phosphorylation levels (Fig. 5A, *top inset*). Expression of constitutively active MEK1 EE abolished the ability of R115,777 to enhance UCN-01 toxicity (Fig. 5A, *bottom*). Athymic mice were injected in the rear flank with MDA-MB-231 cells and tumors were permitted to form. Mice bearing ~100 to 150 mm^3 tumors were then injected i.p. with vehicle, R115,777, UCN-01, or the drug combination for 2 days. Tumor volume was then measured over the following ~30 days. Treatment of mice with either UCN-01 or R115,777 transiently suppressed tumor growth; however, 15 to 30 days following drug exposure, no statistically significant change in tumor volume was noted comparing vehicle-treated, R115,777-treated, or UCN-01-treated tumors (Fig. 5B). In contrast to data obtained following individual drug treatments, combined treatment of animals with R115,777 and UCN-01 significantly reduced tumor growth ($P < 0.05$). In *ex vivo* colony formation assays, 5 and 7 days after the start of drug treatment, tumor cell colony formation was suppressed to a greater extent in cells treated with the drug combination than with either drug individually (Table 4). Of note, although tumor cytoarchitecture was disrupted in drug combination treated tumors in a manner similar to that observed previously in UCN-01- and PD184352-treated tumors, we did not observe a prolonged suppression of basal phosphorylated ERK1/2 levels in studies using the farnesyl transferase inhibitor in combination with UCN-01 (Fig. 5C; cf. Fig. 3C). These findings show that a transient 2-day combined exposure to a clinically relevant farnesyl transferase inhibitor and UCN-01 results in mammary tumor cell killing *in vivo* and long-term suppression of *in vivo* tumor growth.

Discussion

Previous studies by this group have argued that MEK1/2 inhibitors and UCN-01 interact to promote tumor cell-specific killing in a wide variety of malignancies including breast, prostate, and multiple hematologic cell types (22–25). The net output of the cytoprotective RAS-MEK1/2-ERK1/2 pathway has been shown previously to be a critical determinant of tumor cell survival (refs. 20, 21 and references therein). Furthermore, activation of this cascade has been observed as a compensatory response of tumor cells to various environmental stresses, including cytotoxic drugs (20, 21). The present studies were initiated to determine in greater molecular detail than reported previously how MEK1/2 inhibitors interact with UCN-01 to kill mammary carcinoma/substratum attached transformed cells *in vitro*, whether MEK1/2 inhibitor and UCN-01 treatment radiosensitizes mammary tumors *in vitro* and *in vivo*, and whether farnesyl transferase inhibitors interact with UCN-01 to kill mammary carcinoma cells *in vitro* and *in vivo*.

In vitro, based on use of genetic tools, the induction of mitochondrial dysfunction by proteins including BAX and BAK and to a lesser extent BIM and BID was shown to play a primary role in the synergistic induction of cell killing following treatment of cells with MEK1/2 inhibitors and UCN-01. In contrast, in multiple myeloma cells, BIM function was recently shown to be a critical component mediating MEK1/2 inhibitor and UCN-01-stimulated mitochondrial dysfunction and cell killing (34). Based on our findings expressing constitutively active MEK1 EE, a specific activator of ERK1/2, we concluded that the ability of MEK1/2 inhibitors and farnesyl transferase inhibitors to interact with UCN-01 to kill mammary carcinoma cells was due to suppression of the Ras-Raf-MEK-ERK1/2 pathway. Similar data have also been noted in leukemic and myeloma cells (35, 36). We noted that an additional novel clinically relevant MEK1/2 inhibitor, AZD6244, also interacted synergistically with UCN-01 to kill mammary

Downloaded from http://aacrjournals.org/mct/article-pdf/7/3/616/1879092/616.pdf by guest on 07 October 2024

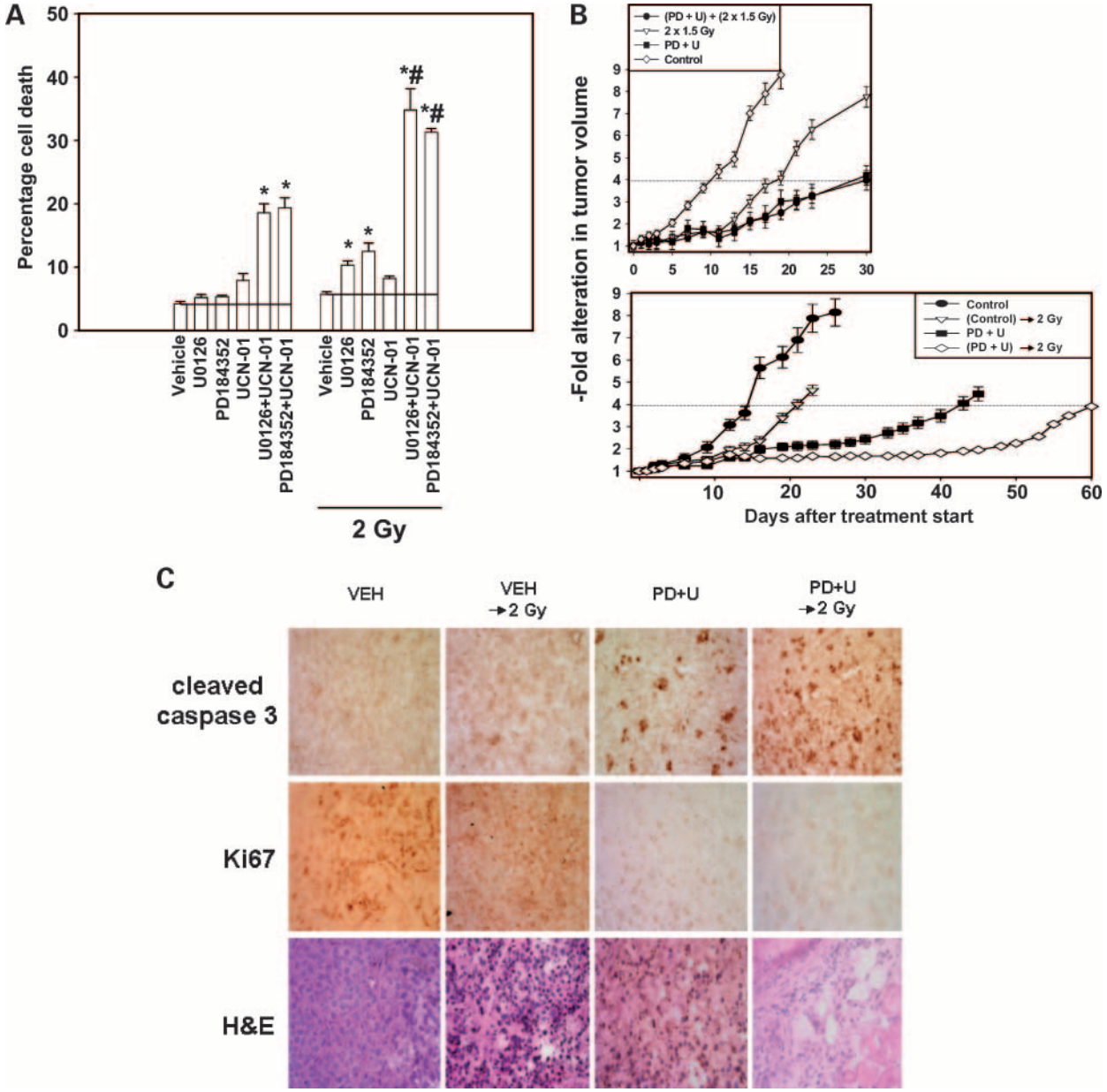

Figure 4. Irradiation of PD184352- and UCN-01-treated tumors following drug treatment has a radiosensitizing effect. **A,** MDA-MB-231 cells were treated with vehicle control (DMSO) or with UCN-01 (150 nmol/L) and the MEK1/2 inhibitors PD184352 or U0126 (1 μmol/L) or UCN-01 and a MEK1/2 inhibitor drug. Following 48 h of drug treatment, medium was carefully removed, the cells were washed, and fresh medium lacking drugs was added to the cultures. Cells were irradiated 24 h after drug removal. Cells were isolated 24 h after irradiation, and the percentage cell death was determined in triplicate from two separate experiments ± SE using trypan blue exclusion assays. **B,** animals were injected 5 million cells/100 μL PBS female athymic mice s.c. into the rear flank: tumor take rate was >90%. Tumors were permitted to form for the following 20 d. Animals with palpable tumors (~100 mm^3) were sorted with the intention of providing a normal distribution of tumor volume within each group, so that the mean tumor volume of all animals within a group was within 10%. Animals were injected with vehicle, PD184352, UCN-01, or the drug combination for 2 d as described in Materials and Methods. Irradiation of the tumors occurred using two different schedules: top, experimental approach 1: two exposures of 1.5 Gy concomitant with drug administration; bottom, experimental approach 2: one exposure of 2 Gy, 24 h after cessation of drug administration. Tumors were calipered to determine their volume calculated as ($width^2$) × length / 2, where width is the smaller of the two measurements. The mean ± SE tumor volume for all animals in each treatment condition was plotted (n = 8 animals per condition). #, $P < 0.05$, less than vehicle control value. Representative of two independent studies per experimental approach. **C,** animals were injected 5 million cells as above and tumors were permitted to form for the following 20 d. Animals with palpable tumors (~100 mm^3) were sorted with the intention of providing a normal distribution of tumor volume within each group, so that the mean tumor volume of all animals within a group was within 10%. Animals were injected with vehicle, PD184352, UCN-01, or the drug combination for 2 d as described in Materials and Methods. Irradiation of the tumors occurred using one exposure of 2 Gy, 24 h after cessation of drug administration. Tumors were removed from animals 7 d after the start of drug exposure. Tumors were fixed and stained with H&E stain to examine tumor cell morphology and using immunohistochemistry to determine the levels of cleaved (active) caspase-3 and Ki67 staining. Representative of two studies.

Downloaded from http://aacrjournals.org/mct/article-pdf/7/3/616/1879092/616.pdf by guest on 07 October 2024

carcinoma cells *in vitro*. Of note, mammary carcinoma cells with very low basal levels of ERK1/2 activity such as MCF7 were apparently as susceptible to being killed by AZD6244 and UCN-01 and were mammary carcinoma cells with very high basal levels of ERK1/2 activity such as MDA-MB-231. *In vivo*, combined exposure of preformed MDA-MB-231 mammary tumors to a MEK1/2 inhibitor or to a farnesyl transferase inhibitor with UCN-01 resulted in a significantly

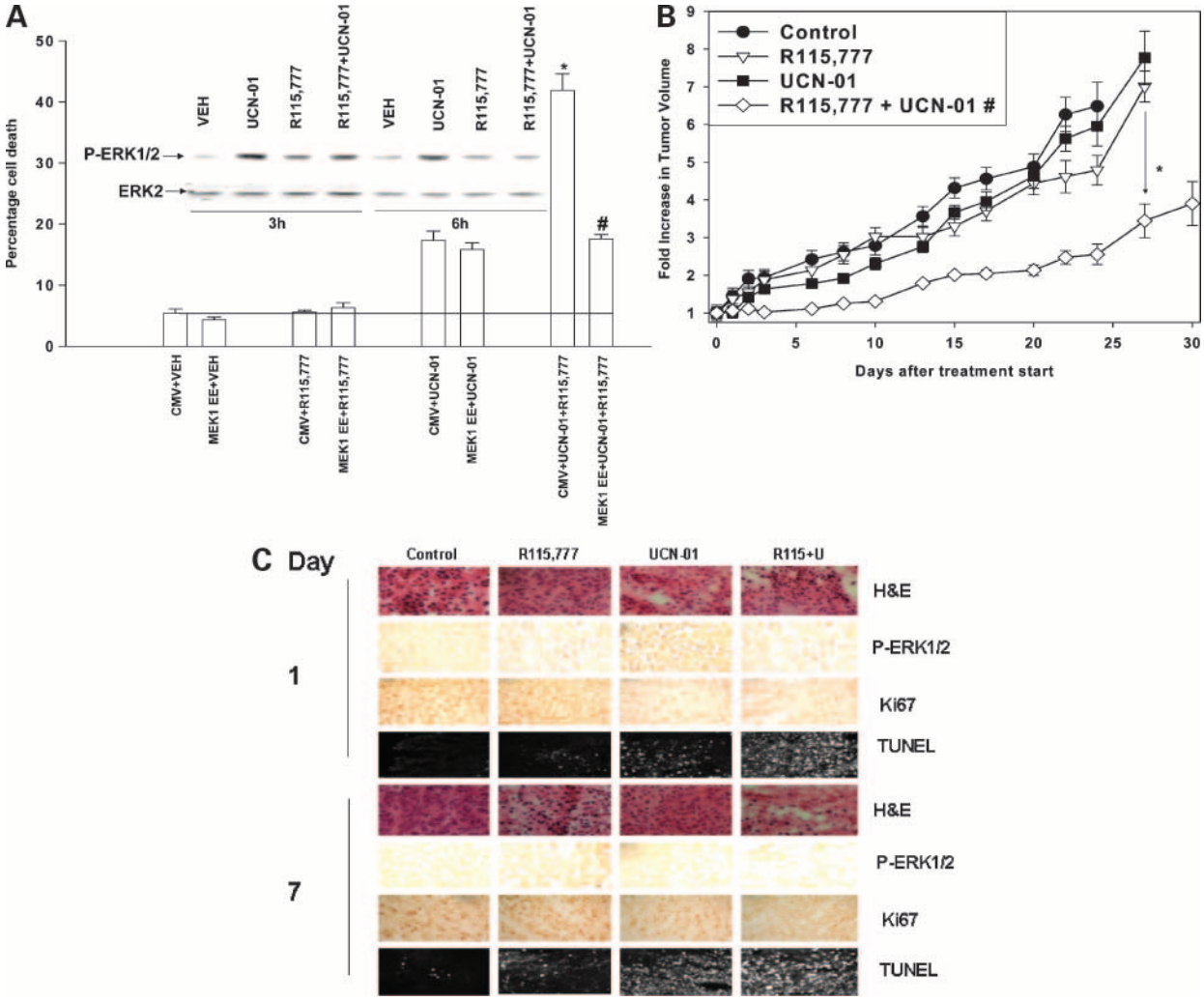

Figure 5. R115,777 and UCN-01 combine kill mammary carcinoma cells *in vitro* and *in vivo*. **A,** MDA-MB-231 cells were cultured as described in Materials and Methods (22). Twelve hours after plating, cells were infected with either a control empty vector adenovirus or an adenovirus to express constitutively active MEK1 EE at a multiplicity of infection of 30. Twenty-four hours after infection, cells were treated with vehicle control (DMSO) or with UCN-01 (150 nmol/L), R115,777 (200 nmol/L), or both drugs. Cells were isolated 48 h after treatment and the percentage cell death was determined in triplicate from two separate experiments ± SE using trypan blue exclusion assays. #, $P < 0.05$, less than corresponding CMV-infected cell value. Top, MDA-MB-231 cells were treated with vehicle control (DMSO) or with UCN-01 (150 nmol/L), R115,777 (200 nmol/L), or both drugs. Cells were isolated at the indicated times after treatment, lysed, and subjected to SDS-PAGE followed by immunoblotting to determine the phosphorylation of ERK1/2 and total ERK2 levels ($n = 3$). **B,** animals were injected 5 million cells/100 μL PBS female athymic mice s.c. into the rear flank: tumor take rate was >90%. Tumors were permitted to form for the following 20 d. Animals with palpable tumors (~100 mm^3) were sorted with the intention of providing a normal distribution of tumor volume within each group, so that the mean tumor volume of all animals within a group was within 10%. Animals were injected with vehicle, UCN-01 (0.2 mg/kg), R115,777 (100 mg/kg), or the drug combination for 2 d as described in Materials and Methods. Tumors were calipered to determine their volume calculated as (width^2) × length / 2, where width is the smaller of the two measurements. The mean ± SE tumor volume for all animals in each treatment condition was plotted ($n = 8$ animals per group). #, $P < 0.05$, less than vehicle control value. Representative of two independent studies. **C,** animals were injected 5 million cells/100 μL PBS female athymic mice s.c. into the rear flank: tumor take rate was >90%. Tumors were permitted to form for the following 20 d. Animals with palpable tumors (~100 mm^3) were sorted with the intention of providing a normal distribution of tumor volume within each group, so that the mean tumor volume of all animals within a group was within 10%. Animals were injected with vehicle, UCN-01 (0.2 mg/kg), R115,777 (100 mg/kg), or the drug combination for 2 d as described in Materials and Methods. Tumors were removed from animals 1 and 7 d after the start of drug exposure. Tumors were fixed and stained with H&E stain and with terminal deoxynucleotidyl transferase–mediated dUTP nick end labeling staining to examine tumor cell morphology and tumor cell death, respectively, and with an anti-phosphorylated ERK1/2 antibody and with an anti-Ki67 antibody to determine the activity of ERK1/2 and measure proliferative index, respectively. Representative of three independent studies.

Downloaded from http://aacrjournals.org/mct/article-pdf/7/3/616/1879092/616.pdf by guest on 07 October 2024

Table 4. R115,777 and UCN-01 act to kill MDA-MB-231 tumor cells growing *in vivo*, as judged using isolated cells in *ex vivo* colony formation assays

Vehicle (day 5)	R115,777	UCN-01	R115,777 + UCN-01
1.00	0.60 ± 0.02	0.51 ± 0.01 (1.00)	0.09 ± 0.01 (0.18*)
Vehicle (day 7)	R115,777	UCN-01	R115,777 + UCN-01
1.00	0.68 ± 0.01	0.75 ± 0.02 (1.00)	0.24 ± 0.02 (0.32*)

NOTE: MDA-MB-231 tumors were treated with R115,777 and UCN-01 as described in Materials and Methods, and 5 or 7 d after the start of drug treatment, the animals were humanely sacrificed and the tumors were isolated. Individual viable MDA-MB-231 cells were isolated from the tumors and then plated in sextuplicate as single cells for colony formation assays as described in Materials and Methods. Colonies were permitted to form for the following 10 to 14 d. Cells were fixed, stained, and counted both manually and using a ColCount machine (Oxford Optronics). The mean ± SE colony numbers from both methods of counting were used to calculate plating efficiency for each treatment condition. Data shown in parentheses indicate cell survival for cells treated with UCN-01, with survival for UCN-01 normalized to 1.00. Data are from a representative experiment (n = 3 separate experiments).
*$P < 0.05$ less than single drug exposure.

Downloaded from http://aacrjournals.org/mct/article-pdf/7/3/616/1879092/616.pdf by guest on 07 October 2024

greater reduction in tumor growth than either drug administered separately that correlated with cleavage of pro-caspase-3 and prolonged suppression of Ki67 immunoreactivity. These observations also correlated with reduced tumor cellularity and *ex vivo* colony formation. Irradiation of tumors following drug exposure, but not concomitantly with drug treatment, enhanced the tumor killing and growth-suppressive effects of MEK1/2 inhibitor and UCN-01 exposure further, arguing that these agents can be effectively combined with established modalities.

The lack of ERK1/2 phosphorylation in MDA-MB-231 tumors treated with UCN-01 and PD184352 several days after cessation of drug treatment was not due to persistence of MEK1/2 inhibitor in the animals/tumors as PD184352-treated tumors showed both suppression of phosphorylated ERK1/2 levels during drug exposure and then a transient rebound in ERK1/2 phosphorylation above levels of control-treated tumors 5 to 10 days following cessation of drug treatment. In addition, it would be unlikely, based on published pharmacokinetic data generated in mice showing UCN-01 had a ~4 to 7 h half-life in rodent plasma, that UCN-01 could have persisted in the MCF7 tumors for ~30 days to alter phosphorylated ERK1/2 levels at this time point (ref. 32 and references therein). Thus, the present findings are most consistent with the notion that tumor cells exposed to both PD184352 and UCN-01 were killed at an early point correlating with drug exposure and that following combined drug treatment these cells were incapable of mounting a compensatory activation of the ERK1/2 pathway to either UCN-01 actions or MEK1/2 inhibition, thereby resulting in a prolonged suppression of tumor re-growth.

In contrast to our data with the MEK1/2 inhibitor PD184352, treatment of MDA-MB-231 cells *in vitro* or grown as tumors with the farnesyl transferase inhibitor R115,777 did not suppress basal levels of ERK1/2 phosphorylation, although *in vitro* and *in vivo* this agent blunted UCN-01-induced ERK1/2 phosphorylation. This, in part, could be explained because MDA-MB-231 cells express mutated active K-RAS V12, which is geranylgeranylated and whose function and downstream enhancing effects on ERK1/2 phosphorylation are unlikely to be significantly inhibited by farnesyl transferase inhibitors. Furthermore, in tumors treated with R115,777 and UCN-01, the levels of ERK1/2 phosphorylation remained at near control levels several days after drug administration unlike data using PD184352. However, *in vivo* tumor growth data and *ex vivo* colony formation data showed that tumor cell killing had occurred in R115,777- and UCN-01-treated animals. Collectively, our findings suggest that transient or prolonged suppression of basal ERK1/2 activity may not be the key process by which R115,777, and possibly PD184352, act to enhance UCN-01 lethality but that blockade of UCN-01-stimulated activation of ERK1/2 function during the 48 h of drug exposure, at the levels of RAS proteins or MEK1/2, may be the primary mechanism responsible for cell killing.

In published studies treating animals with either UCN-01 or PD184352 as individual agents, noticeably higher drug concentrations than those used herein have been administered to show significant antitumor effects. For example, Gao et al. treated animals carrying head and neck tumor xenografts for 5 days with 7.5 mg/kg UCN-01 to achieve tumor regression (28). Similarly, Sebolt-Leopold et al. and McDaid et al. used PD184352 concentrations in the 48 to 300 mg/kg range (with drug administration over each of ~14-20 days) to achieve antitumor effects (37, 38). The maximal free concentration of PD184352 in many patients based on phase I/II clinical trail data appears to be in the range ~400 nmol/L, which is due in part to the rapid metabolism of this drug in patients (39, 40). A 25 mg/kg dosing of PD184352 results in a theoretical peak concentration of 50 μmol/L. Due to poor pharmacokinetic properties, PD184352 is no longer under clinical investigation.

Based on initial phase I studies, the maximal free achievable concentration of UCN-01 in human plasma was thought to be at or below ~100 nmol/L with a long plasma half-life due to UCN-01 binding to human α1 acidic glycoprotein, which is a considerably lower concentration than that achievable in rodent plasma (41–43). The clinical utility of UCN-01 was limited due to its binding to α1 acidic glycoprotein and also to the possibility that off-target

actions may be responsible for toxicity, such as hyperglycemia (44). A novel UCN-01 schedule has recently been developed in which UCN-01 is administered as a 3-h infusion (95 mg/m^2) q3w (45). This schedule, which appears to be well tolerated, results in free, salivary UCN-01 plasma concentrations of 800 to 1,400 nmol/L, which are sustained for up to 3 weeks following drug administration. Combination of the new UCN-01 schedule with topotecan or cisplatin has shown preliminary evidence of patient activity (46, 47). In our animal studies, the theoretical peak UCN-01 concentration for treatment of mammary tumors with the drug, based on instantaneous absorption of the entire agent, would be in the range of ~300 nmol/L. Thus, the concentrations of UCN-01 used in our studies are within the clinically achievable range. In the case of MEK1/2 inhibitors, newer second-generation MEK1/2 inhibitors, such as AZD6244, have been developed, which display superior pharmacokinetic characteristics in humans compared with PD184352 (48). We have found *in vitro* that AZD6244 behaves in a nearly identical manner to PD184352 with respect to enhancing UCN-01 lethality in MCF7 and MDA-MB-231 cells (and transformed fibroblasts), and further studies will be required to determine whether AZD6244 enhances UCN-01 lethality in mammary carcinoma xenograft tumors.

The abrogation of the G_2-M cell cycle checkpoint has in general been linked *in vitro* to the radiosensitization and chemosensitization properties attributed to UCN-01 (e.g., refs. 3, 4, 6). Previous studies by our laboratory had noted that irradiation of mammary and prostate carcinoma cells concomitant with MEK1/2 inhibitor and UCN-01 exposure did not significantly enhance short-term cell killing and only modestly reduced clonogenic survival (22). Our present analyses showed both *in vitro* and *in vivo* that irradiation of mammary tumor cells/tumors following MEK1/2 inhibitor and UCN-01 exposure resulted in a profound radiosensitization of the tumor cells/tumors that correlated with increased cell killing and reduced tumor re-growth. At present, the mechanisms by which this sensitization occurs are unclear. Several possible mechanisms for this observation appear probable: (*a*) as cells recover from MEK1/2 inhibitor and UCN-01 exposure, they reenter the cell cycle and become more susceptible to the toxic effects of ionizing radiation exposure than growth-arrested cells and (*b*) surviving cells treated with MEK1/2 inhibitors and UCN-01 have damaged or dysfunctional mitochondria, which make them more susceptible to subsequent ionizing radiation exposure. Future studies will be required to clarify the precise mechanisms by which MEK1/2 inhibitors and UCN-01 radiosensitize mammary tumor cells in a sequence-dependent manner. In conclusion, it will be of future interest to determine whether the effects observed in our studies can be translated into the clinical arena.

References

1. Mow BM, Blajeski AL, Chandra J, Kaufmann SH. Apoptosis and the response to anticancer therapy. Curr Opin Oncol 2001;13:453 – 62.

2. Mizuno K, Noda K, Ueda Y, et al. UCN-01, an anti-tumor drug, is a selective inhibitor of the conventional PKC subfamily. FEBS Lett 1995; 359:259 – 61.

3. Graves PR, Yu L, Schwarz JK, et al. The Chk1 protein kinase and the Cdc25C regulatory pathways are targets of the anticancer agent UCN-01. J Biol Chem 2000;275:5600 – 5.

4. Peng C-Y, Graves PR, Thoma RS, et al. Mitotic and G_2 checkpoint control: regulation of 14-3-3 protein binding by phosphorylation of Cdc25C on serine-216. Science 1997;277:1501 – 5.

5. Komander D, Kular GS, Bain J, Elliott M, Alessi DR, Van Aalten DM. Structural basis for UCN-01 (7-hydroxystaurosporine) specificity and PDK1 (3-phosphoinositide-dependent protein kinase-1) inhibition. Biochem J 2003;375:255 – 62.

6. Busby EC, Leistritz DF, Abraham RT, Karnitz LM, Sarkaria JN. The radiosensitizing agent 7-hydroxystaurosporine (UCN-01) inhibits the DNA damage checkpoint kinase hChk1. Cancer Res 2000;60:2108 – 211.

7. Bunch RT, Eastman A, Enhancement of *cis*-platinum-induced cytotoxicity by 7-hydroxystaurosporine, a new G_2 checkpoint inhibitor. Clin Cancer Res 1996;2:791 – 7.

8. Tang L, Boise LH, Dent P, Grant S. Potentiation of 1-β-D-arabinofuranosylcytosine-mediated mitochondrial damage and apoptosis in human leukemia cells (U937) overexpressing bcl-2 by the kinase inhibitor 7-hydroxystaurosporine (UCN-01). Biochem Pharmacol 2000;60:1445 – 56.

9. Shao R-G, Cao C-X, Shimizu T, et al. Abrogation of an S-phase checkpoint and potentiation of camptothecin cytotoxicity by 7-hydroxystaurosporine (UCN-01) in human cancer cell lines, possibly influenced by p53 function. Cancer Res 1997;57:4029 – 35.

10. Wang Q, Worland PJ, Clark JL, Carlson BA, Sausville EA. Apoptosis in 7-hydroxystaurosporine-treated T lymphoblasts correlates with activation of cyclin-dependent kinases 1 and 2. Cell Growth Differ 1995;6: 927 – 36.

11. Tombes R, Auer KL, Mikkelsen R, et al. The mitogen-activated protein (MAP) kinase cascade can either stimulate or inhibit DNA synthesis in primary cultures of rat hepatocytes depending upon whether its activation is acute/phasic or chronic. Biochem J 1998;330:1451 – 60.

12. Park JS, Boyer S, Mitchell K, et al. Expression of human papilloma virus E7 protein causes apoptosis and inhibits DNA synthesis in primary hepatocytes via increased expression of p21$^{Cip\text{-}1/WAF1/mda6}$. J Biol Chem 2000;274:18 – 28.

13. Vrana J, Grant S, Dent P. MAPK and JNK1 activities in HL-60 cells over-expressing Bcl-2 after exposure to ionizing radiation; possible roles of these pathways in leukemic cell survival. Radiation Res 1999;151: 559 – 69.

14. Hayne C, Tzivion G, Luo Z. Raf-1/MEK/MAPK pathway is necessary for the G_2-M transition induced by nocodazole. J Biol Chem 2000;275: 31876 – 82.

15. Carter S, Auer KL, Birrer M, et al. Potentiation of ionizing radiation induced cell killing by inhibition of the mitogen activated protein (MAP) kinase cascade in A431 human squamous carcinoma cells. Oncogene 1998;16:2787 – 96.

16. Jarvis WD, Fornari FA, Tombes RM, et al. Chemo-potentiation of 1-β-D-arabino-furanosylcytosine-related cytotoxicity in human myeloid leukemia cells by pharmacological modulation of protein kinase C and mitogen-activated protein kinase. Mol Pharmacol 1998;54:844 – 56.

17. Wang S, Guo CY, Dent P, Grant S. Effect of Bcl-XL expression on Taxol-induced apoptosis and cytotoxicity in human leukemia cells (U937). Leukemia 1999;13:1564 – 73.

18. Park JS, Reardon DB, Carter S, et al. Mitogen activated protein (MAP) kinase pathway signaling is required for release/progression of cells through G_2-M after exposure to ionizing radiation. Mol Biol Cell 1999;10: 4215 – 31.

19. Wang Z, VanTuyle G, Conrad D, et al. Dysregulation of the cyclin dependent kinase inhibitor p21 WAF1/CIP1/MDA6 increases the susceptibility of human leukemia cells (U937) to 1-β-D-arabinofuranosylcytosine-mediated mitochondrial dysfunction and apoptosis. Cancer Res 1999;59: 1259 – 67.

20. Dent P, Yacoub A, Fisher PB, Hagan MP, Grant S. MAPK pathways in radiation responses. Oncogene 2003;22:5885 – 96.

21. Dent P, Qiao L, Grant S. Signaling by ErbB family receptors. Front Biosci 2002;7:D376 – 89.

22. McKinstry R, Qiao L, Yacoub A, et al. Pharmacologic inhibitors of the mitogen activated protein kinase cascade interact synergistically with UCN-01 to induce mitochondrial dysfunction and apoptosis in mammary and prostate carcinoma cells. Cancer Biol Ther 2002;1:241 – 51.

Downloaded from http://aacrjournals.org/mct/article-pdf/7/3/616/1879092/616.pdf by guest on 07 October 2024

23. Dai Y, Decker RH, McKinstry R, Dent P, Grant S. Pharmacologic inhibitors of the mitogen activated protein kinase cascade interact synergistically with UCN-01 to induce mitochondrial dysfunction and apoptosis in leukemia and lymphoma cells. Cancer Res 2001;61:5106 – 15.

24. Dai Y, Landowski TH, Rosen ST, Dent P, Grant S. Combined treatment with the checkpoint abrogator UCN-01 and MEK1/2 inhibitors potently induces apoptosis in drug-sensitive and -resistant myeloma cells through an IL-6-independent mechanism. Blood 2002;100:3333 – 43.

25. Yu C, Dai Y, Dent P, Grant S. Coadministration of UCN-01 with MEK1/2 inhibitors potently induces apoptosis in BCR/ABL + leukemia cells sensitive and resistant to ST1571. Cancer Biol Ther 2002;1:674 – 82.

26. Dai Y, Rahmani M, Pei XY, et al. Farnesyltransferase inhibitors interact synergistically with the Chk1 inhibitor UCN-01 to induce apoptosis in human leukemia cells through interruption of both Akt and MEK/ERK pathways and activation of SEK1/JNK. Blood 2005;105: 1706 – 16.

27. Yu C, Rahmani M, Dai Y, et al. The lethal effects of pharmacological cyclin-dependent kinase inhibitors in human leukemia cells proceed through a phosphatidylinositol 3-kinase/Akt-dependent process. Cancer Res 2003;63:1822 – 33.

28. Gao N, Dai Y, Rahmani M, Dent P, Grant S. Contribution of disruption of the nuclear factor-κB pathway to induction of apoptosis in human leukemia cells by histone deacetylase inhibitors and flavopiridol. Mol Pharmacol 2004;66:956 – 63.

29. Rahmani M, Reese E, Dai Y, et al. Coadministration of histone deacetylase inhibitors and perifosine synergistically induces apoptosis in human leukemia cells through Akt and ERK1/2 inactivation and the generation of ceramide and reactive oxygen species. Cancer Res 2005;65: 2422 – 32.

30. Yu C, Krystal G, Varticovksi L, et al. Pharmacologic mitogen-activated protein/extracellular signal-regulated kinase kinase/mitogen-activated protein kinase inhibitors interact synergistically with STI571 to induce apoptosis in Bcr/Abl-expressing human leukemia cells. Cancer Res 2002; 62:188 – 99.

31. Brust D, Feden J, Farnsworth J, Amir C, Broaddus WC, Valerie K. Radiosensitization of rat glioma with bromodeoxycytidine and adenovirus expressing herpes simplex virus-thymidine kinase delivered by slow, rate-controlled positive pressure infusion. Cancer Gene Ther 2000;7: 778 – 88.

32. Dai Y, Khanna P, Chen S, Pei XY, Dent P, Grant S. Statins synergistically potentiate 7-hydroxystaurosporine (UCN-01) lethality in human leukemia and myeloma cells by disrupting Ras farnesylation and activation. Blood. Epub ahead of print 2007.

33. Pei XY, Dai Y, Rahmani M, Li W, Dent P, Grant S. The farnesyltransferase inhibitor L744832 potentiates UCN-01-induced apoptosis in human multiple myeloma cells. Clin Cancer Res 2005;11:4589 – 600.

34. Pei XY, Dai Y, Tenorio S, et al. MEK1/2 inhibitors potentiate UCN-01 lethality in human multiple myeloma cells through a Bim-dependent mechanism. Blood. Epub ahead of print 2007.

35. Pei XY, Li W, Dai Y, Dent P, Grant S. Dissecting the roles of checkpoint kinase 1/CDC2 and mitogen-activated protein kinase kinase 1/2/extracellular signal-regulated kinase 1/2 in relation to 7-hydroxystaurosporine-induced apoptosis in human multiple myeloma cells. Mol Pharmacol 2006;70:1965 – 73.

36. Dai Y, Khanna P, Chen S, Pei XY, Dent P, Grant S. Statins synergistically potentiate 7-hydroxystaurosporine (UCN-01) lethality in human leukemia and myeloma cells by disrupting Ras farnesylation and activation. Blood 2007;109:4415 – 23.

37. Sebolt-Leopold JS, Dudley DT, Herrera R, et al. Blockade of the MAP kinase pathway suppresses growth of colon tumors *in vivo*. Nat Med 1999;5:810 – 6.

38. McDaid HM, Lopez-Barcons L, Grossman A, et al. Enhancement of the therapeutic efficacy of Taxol by the mitogen-activated protein kinase kinase inhibitor CI-1040 in nude mice bearing human heterotransplants. Cancer Res 2005;65:2854 – 60.

39. Rinehart J, Adjei AA, Lorusso PM, et al. Multicenter phase II study of the oral MEK inhibitor, CI-1040, in patients with advanced non-small-cell lung, breast, colon, and pancreatic cancer. J Clin Oncol 2004;22: 4456 – 62.

40. Lorusso PM, Adjei AA, Varterasian M, et al. Phase I and pharmacodynamic study of the oral MEK inhibitor CI-1040 in patients with advanced malignancies. J Clin Oncol 2005;23:5281 – 93.

41. Sausville EA, Lush RD, Headlee D, et al. Clinical pharmacology of UCN-01: initial observations and comparison to preclinical models. Cancer Chemother Pharmacol 1998;42 Suppl:S54 – 9.

42. Fuse E, Tanii H, Kurata N, et al. Unpredicted clinical pharmacology of UCN-01 caused by specific binding to human α1-acid glycoprotein. Cancer Res 1998;58:3248 – 53.

43. Hagenauer B, Maier-Salamon A, Thalhammer T, Zollner P, Senderowicz A, Jager W. Metabolism of UCN-01 in isolated perfused rat liver: role of Mrp2 in the biliary excretion of glucuronides. Oncol Rep 2004;11:1069 – 75.

44. Fuse E, Kuwabara T, Sparreboom A, Sausville EA, Figg WD. Review of UCN-01 development: a lesson in the importance of clinical pharmacology. J Clin Pharmacol 2005;45:394 – 403.

45. Dees EC, Baker SD, O'Reilly S, et al. A phase I and pharmacokinetic study of short infusions of UCN-01 in patients with refractory solid tumors. Clin Cancer Res 2005;11:664 – 71.

46. Hotte SJ, Oza A, Winquist EW, et al. Phase I trial of UCN-01 in combination with topotecan in patients with advanced solid cancers: a Princess Margaret Hospital Phase II Consortium study. Ann Oncol 2006; 17:334 – 40.

47. Perez RP, Lewis LD, Beelen AP, et al. Modulation of cell cycle progression in human tumors: a pharmacokinetic and tumor molecular pharmacodynamic study of cisplatin plus the Chk1 inhibitor UCN-01 (NSC 638850). Clin Cancer Res 2006;12:7079 – 85.

48. Yeh TC, Marsh V, Bernat BA, et al. Biological characterization of ARRY-142886 (AZD6244), a potent, highly selective mitogen-activated protein kinase kinase 1/2 inhibitor. Clin Cancer Res 2007;13:1576 – 83.

Downloaded from http://aacrjournals.org/mct/article-pdf/7/3/616/1879092/616.pdf by guest on 07 October 2024